Short communication

Lithium intercalation characteristics of B–C–N and C–B–Si–N carbon alloys

H. Huang[*], E.M. Kelder, J. Schoonman

Laboratory for Inorganic Chemistry, Delft Interfaculty Research Center: Renewable Energy,
Delft University of Technology, Julianalaan 136, 2628BL Delft, The Netherlands

Abstract

The possibility of the application of B–C–N and C–B–Si–N carbon alloys as anode materials for Li-ion batteries is discussed. The structure, composition, and the electrochemical behavior of these materials are presented. B–C–N samples prepared by the high-pressure self-combustion sintering technique are found to be a mixture of hexagonal BN and partly crystallized ''BCN'' compounds. Li-ions can be intercalated into the structure electrochemically with a maximum reversible capacity of about 120 mAh/g. For a C–B–Si–N carbon alloy, a reversible capacity of 500 mAh/g can be obtained at a low current rate, which is higher than that of the pure carbon pitch heated at the same temperature. © 2001 Elsevier Science B.V. All rights reserved.

Keywords: Carbon alloy; BCN compounds; Intercalation; Li-ion battery; Anode

1. Introduction

The incorporation of foreign atoms, especially the immediate neighbors in the Periodic Table, such as N, B, and Si into carbon is a current subject of interest in carbon chemistry. It is often referred to as a carbon alloy. Carbon alloying with other elements which are homogeneously dispersed in the carbon network has more potential applicability than pure carbon. For the development of Li-ion batteries much effort has been focused on new or improved materials. Work on the anode side has been mostly on carbon materials. The interesting influences of dopant elements in the carbon covalent network were recently reported. Phosphorous doped carbon increased the capacity substantially [1]. Substituting carbon by an appropriate amount of boron atoms was found to increase the reversible capacity, as well as the intercalation potential [2]. Although, nitrogen-containing carbons showed large irreversible capacity and low cycleability [3], surface modification with nitrogen was reported to improve the performance of carbon [4]. Morita et al. published their results on Li intercalation characteristics of BC_xN ($x = 2, 3, 7,$ and 10) since 1992 [5,6]. This raised a particular interest as ''BCN'' compounds have a very similar structure to graphite. It is reported that BCN compounds with various bandgap energies can be predicted theoretically by controlling the B, C, N atomic composition and atomic arrangement [7]. Hence, from a fundamental point of view, it is very interesting to study lithium intercalation mechanisms into these layered compounds. Recently using high-pressure self-combustion sintering technique a series of ''BCN'' compounds were synthesized [8] and the electrochemical measurements were carried out [9] to provide more experimental data for future theoretical analyses. C–B–Si–N carbon alloys were reported to have a better resistance to oxidation compared with pure carbon fibers. These materials even maintain their fibrous morphology after treatment at 2800°C [10]. It was prepared via co-pyrolysis of B, N, Si, and pitch precursors and the structure is believed to consist of planar polyaromatic units grafted with fragments containing B, N, and Si, which determine its possible combination of the properties of C_xB, C_xN, and C_xSi. Little is known about the lithium intercalation characteristics of this kind of carbon alloy. Hence, our recent results on the intercalation characteristics of Li into these two kinds of carbon alloys will be presented.

2. Experimental aspects

Synthesis of BCN compounds was realized using the high-pressure self-combustion sintering (HPCS) technique.

---

[*] Corresponding author. Tel.: +31-15-2783891; fax: +31-15-2788047.
E-mail address: h.huang@tnw.tudelft.nl (H. Huang).

Table 1
Specification, composition, and specific surface area of BCN compounds

Samples	Nominal composition (at%)			S (m^2/g), BET data
	C	B	N	
BCN01	25	37	38	
BCN02	40	30	30	12
BCN03	45	25	30	17
BCN04	52	22	26	21
BCN05	60	22	18	19

The reactants, i.e. $B_2O_3(OH)_x$, polyethylene $(C_2H_2)_n$ or propylene $(C_3H_3)_n$, were treated at the combustion regime (1800°C) in a high-pressure (nitrogen 100 atm) chemical reactor. The reactor contains a high-pressure and heating-control system and ignition units [8]. The specifications and compositions of the prepared B–C–N samples are listed in Table 1. The specific surface area, S was obtained using the BET method.

The C–B–Si–N carbon alloys were prepared via co-pyrolysis of a light fraction of Ashland A240 petroleum pitch with polydimethylsilane, followed by co-pyrolysis of the product with borane, pyridine and heat treatment in nitrogen at 1200°C. The composition is approximately B 5 mass%, Si 15 mass%, N 10 mass%, and C 70 mass% [10].

The structure of the samples was analyzed by XRD on a Philips PW1840 X-ray diffractometer with Cu Kα radiation. FTIR spectra were obtained on a Perkin-Elmer apparatus (FTIR Spectrometer 1000) using the KBr disc method.

The electrodes for the electrochemical measurements were prepared by doctor-blade coating on copper foils. A slurry was made by mixing the carbon-alloy samples with polyacrylonitrile (PAN)-based binder (95:5 by weight) with dimethyl formamide (DMF) as the solvent. After pressing and drying at 150°C for 3 h in air, the samples were dried subsequently at 100 C for 24 h in vacuum. The as-prepared electrode foils were transferred to a glove box filled with He gas. Finally, the state-of-the-art two electrode cells were assembled with 1 M-LiPF$_6$–EC–EMC (ethylene carbonate and ethyl-methyl carbonate) as electrolyte and fresh Li foils as both reference and counter electrodes. The samples were discharged and charged at a constant current rate in the voltage range of 5 mV to 2.5 V. The voltage of the cells was monitored as a function of time. Then the discharge/charge capacities were calculated from the current, the mass of the cathode, and the step time. All the measurements were controlled and recorded automatically by a Maccor battery tester.

3. Results and discussion

3.1. BCN compounds

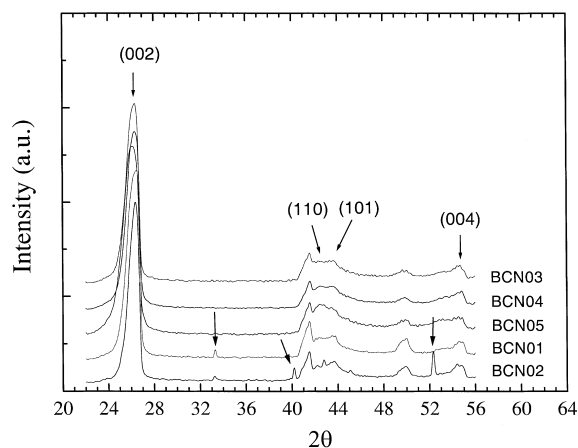Fig. 1 shows the XRD spectra of all the prepared B–C–N samples. The positions of all the diffraction peaks are

Fig. 1. XRD spectra of the synthesized BCN samples.

consistent with the h-BN and ''BCN'' phases indicating that the samples are in fact a mixture of h-BN and ''BCN'' compounds. For samples BCN01 and BCN02 some additional peaks neither belonging to h-BN nor to ''BCN'' were observed in the XRD spectra and possibly correspond to boron carbide.

It is apparent that in the scan region of 40–47° of the XRD spectra the multipeaks for all the samples indicate 3D ordering. Dahn et al. [11] reported and analyzed the XRD powder diffraction profiles of pyrolyzed carbon at different temperatures in detail. According to their results, petroleum pitch heated below 2000°C consisted to a large extent of turbostratic carbon with negligible 3D ordering. Only at 2100°C, a shoulder on the right side of (10) peak near 43° begins to develop indicating the relief of turbostratic disorder. In our samples prepared at only 1800°C, the presence of the multipeaks indicating 3D ordering in the structure probably is the result of doping with B and N atoms.

As the (0 0 2) diffraction peaks corresponding to h-BN and ''BCN'' phases overlap, it is more convenient to focus on the details of the multipeaks in the range of 40–47° in order to obtain more information about the synthesized ''BCN'' materials. From JCPDS data, the peak at 41.6° corresponds to the (1 1 0) diffraction from h-BN, while the peak at 42.4° is from ''BCN''. The intensity ratio between the two fingerprint diffraction peaks at 41.6 and 42.4° is determined by the mass ratio of h-BN and ''BCN'' in the samples. Qualitatively, it means that the larger the content of ''BCN'', the higher will be the intensity of the peak at 42.4°. Therefore, BCN05 has the highest content of ''BCN'', samples BCN04 has a mediate ''BCN'' content, while BCN03 contains the least ''BCN'' of the present samples.

Fig. 2(a) shows the first discharge/charge profiles at a current density of 0.1 mA/cm^2. It can be seen that both the charge/discharge efficiency (Eff.) and the reversible capacity (Q_r) increased in the sequence BCN03, BCN04, and BCN05 with increasing the amount of active ''BCN'' compound. When the cells were discharged/charged at a lower current density, i.e. $I = 0.01$ mA/cm^2, an increase of the reversible
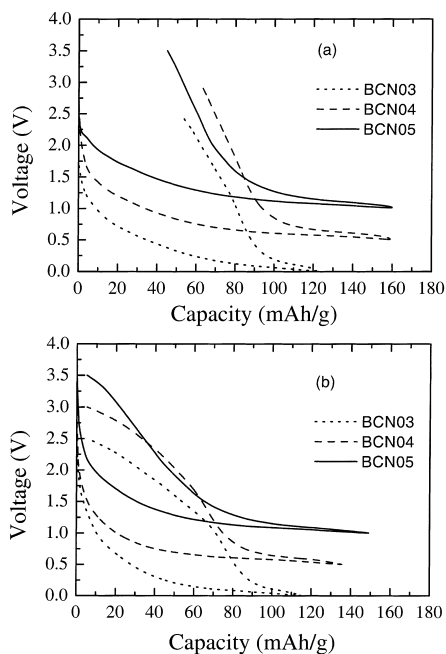
Fig. 2. The discharge/charge profiles of the prepared "BCN" compounds: (a) the first cycle at a current density of 0.1 mA/cm^2; (b) the 5th cycle at a current density of 0.01 mA/cm^2 (for better resolution, the curves for samples BCN05 and BCN04 are shifted 1.0 and 0.5 V, respectively).

capacity was observed, still with the largest value for sample BCN05 (Fig. 2(b)). In the Table 2, both the irreversible capacity (Q_{ir}) and reversible capacity (Q_r) data as well as the first charge/discharge efficiency (Eff.) are presented.

As can be seen in Fig. 2 and Table 2, sample BCN05 has the lowest irreversible capacity and the highest reversible capacity, which can be attributed to the existence of the smallest amount of the inactive h-BN phase. Apart from the reason that the specific capacity is calculated according to the total mass of the sample, h-BN is an insulator with a bandgap of 5.2 eV. Hence, the existence of BN does not facilitate electronic conductivity resulting in a large potential polarization.

Comparing with the results of Morita et al. [5], the results from the present samples are very different; here lithium can be intercalated/de-intercalated reversibly at low potentials (below 500 mV). This characteristic is similar to that of soft carbon heated at around 2000°C, in which capacity shifted also to the lower voltage region by appearance of a plateau

Table 2
Comparison of irreversible and reversible capacity in terms of mAh/g of the B–C–N compounds with different compositions[a]

Samples	$I = 0.1$ mA/cm^2			$I = 0.01$ mA/cm^2		
	Q_{ir}	Q_r	Efficiency (%)	Q_{ir}	Q_r	Efficiency (%)
BCN03	52	70	57	80	110	58
BCN04	62	97	61	85	130	60
BCN05	45	115	72	60	144	71

[a] Efficiency = $Q_r/(Q_{ir} + Q_r)$.

near 0.1 V due to the transformation of the turbostratic structure to a 3D ordered structure. Accordingly, the different lithium intercalation characteristics are attributed to the higher degree of 3D ordering in the present samples compared to those studied by Morita et al.

3.2. C–B–Si–N compound

The FTIR spectrum of C–B–Si–N reveals the carbon atoms to be bonded with the dopant atoms, the peaks at 3413, 1092 and 782 cm^{-1} correspond to specific bond vibrations of C–N, C–B, and C–Si, respectively (see Fig. 3) [12]. The other peaks correspond to the C–C and C–H vibrations. The XRD spectrum of this compound is shown in Fig. 4. The broad peak at around 43° is due to the honeycomb structure of small graphene sheets showing that most of the carbon is present in an sp^2-bonded configuration. The broad peak at around 25° indicates that there is little parallel stacking of the graphene sheets [11]. This pattern is similar to that of turbostratic carbon. Considering the sample's stoichiometry and combining with the FTIR results, the structure of this material is believed to consist of planar
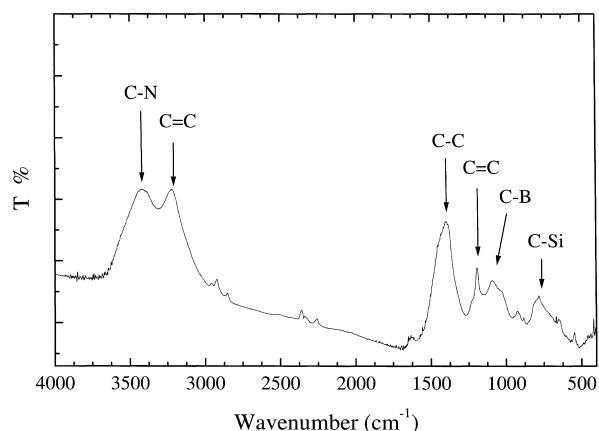

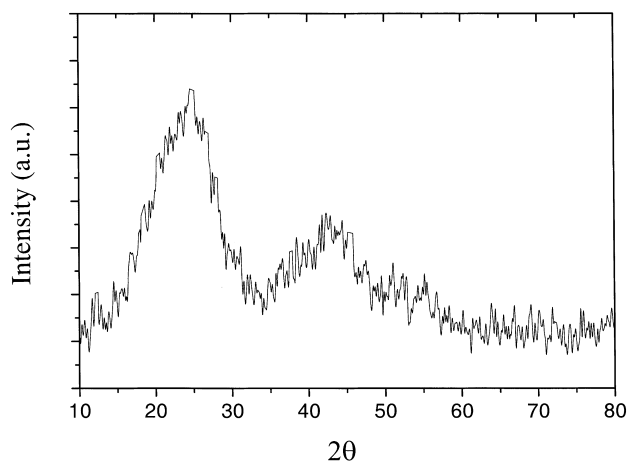Fig. 3. The FTIR spectrum of the C–B–Si–N compound.

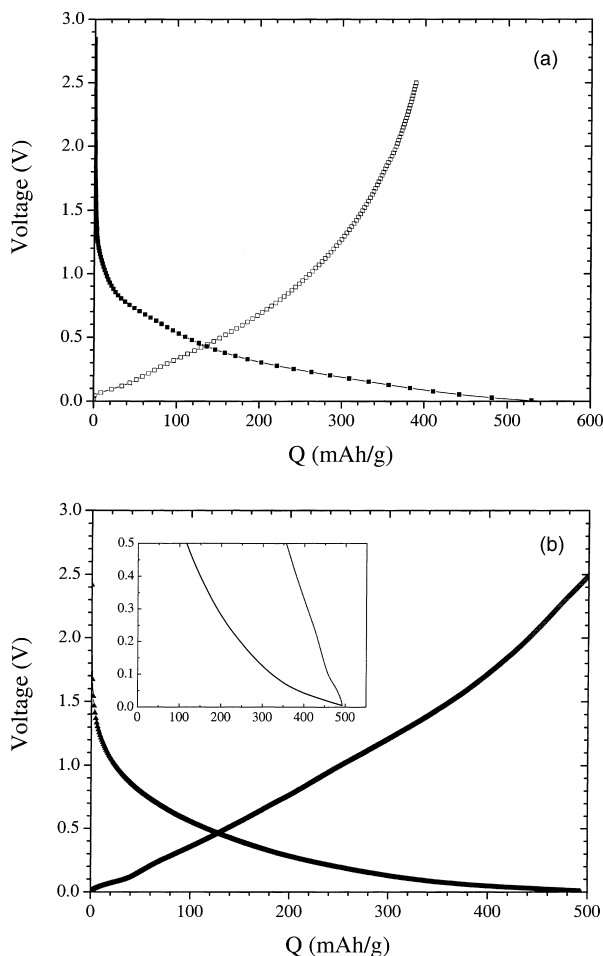Fig. 4. The XRD spectrum of the C–B–Si–N compound.

Fig. 5. (a) The 1st discharge/charge profile of the C–B–Si–N compound, $I = 0.1$ mA/cm^2; (b) the 4th discharge/charge profile of C–B–Si–N compound, $I = 0.01$ mA/cm^2.

polyaromatic units from the A240 pitch with polydimethyl-silane, borane, and pyridine fragments grafted on these units. This grafting disrupts the planar structure and prevents the occurrence of the graphite structure.

Fig. 5(a) showed the first discharge/charge profile at a current density of 0.1 mA/cm^2. The irreversible capacity and reversible capacity are 140 and 390 mAh/g, respectively. After three cycles, the discharge/charge current density was lowered to 0.01 mA/cm^2. At this low current rate, the reversible capacity increased to 500 mAh/g (see Fig. 5(b)), which is much larger than that of a pure carbon pitch heated at 1200°C. A small plateau below 0.1 V can be observed from the inset in Fig. 5(b), which is probably related to a certain reaction between Li and Si grafting on the carbon sheets. On the other hand, a larger voltage hysteresis (about 0.55 V) is observed as compared to pure silicon-containing carbon (0.39 and 0.34 V for samples G and N, respectively, in [13]). This is possibly related to the B or N atoms in the carbon alloy as those lead to insulating regions, and hence, high potential polarization.

4. Conclusions

The BCN samples prepared by the high-pressure self-combustion sintering technique (HPCS) are mixtures of h-BN and partly crystallized "BCN". Li ions can be inter-calated/de-intercalated into the "BCN" compounds electro-chemically with a maximum reversible capacity of about 150 mAh/g. The obtained low value is due to the existence of inactive impurity phases, e.g. h-BN. More lithium ions are expected to be intercalated reversibly in the case of pure crystallized "BCN". Care much be taken to avoid h-BN formation as this highly insulating inactive material leads to large internal potential polarization.

C–B–Si–N carbon alloy is found to be suitable for lithium intercalation/de-intercalation. The first charge/discharge efficiency is 73%. When charging/discharging at a low current rate, the reversible capacity is 500 mAh/g, higher than that of the pure carbon pitch heated at the same temperature. With proper adjustment of the C, B, N, Si stoichiometry in the compound, it is expected that the advantages of C_xB, C_xN, and C_xSi can be combined in order to improve capacity and performance of such anode materials for rechargeable lithium-ion batteries.

Acknowledgements

References

[1] A. Omaru, H. Azuma, N. Aoki, A. Kita, Y. Nishi, Extended Abstr., in: the Proceedings of the 182nd meeting of the Electrochemical Society, Toronto, Canada, 1992.
[2] B.M. Way, J.R. Dahn, J. Electrochem. Soc. 141 (1994) 907.
[3] W.J. Weydanz, B.M. Way, T. van Buuren, J.R. Dahn, J. Electrochem. Soc. 141 (1994) 900.
[4] T. Nakajima, M. Koh, Denki Kagaku 64 (1996) 917.
[5] M. Morita, H. Hanada, T. Tsutsumi, Y. Matsuda, M. Kawaguchi, J. Electrochem. Soc. 139 (1991) 1227.
[6] M. Ishikawa, T. Nakamura, M. Morita, Y. Matsuda, S. Tsujioka, T. Kawashima, J. Power Sources 55 (1995) 127.
[7] A.Y. Liu, R.M. Wentzcovitch, M.L. Cohen, Phys. Rev. B 39 (1989) 1760.
[8] J. Schoonman, Y. Frolov, A. Ivanov-Schitz, Novel ion and mixed conductors for solid state ionic devices: synthesis based on combustion wave and shock wave methods, INTAS final Report, 1996.
[9] A. Westwood, Private communication.
[10] H. Huang, Anode materials for Li-ion Batteries, PhD thesis, Delft University of Technology, Universal Press, Veenendaal, The Nether-lands, 1999.
[11] J.R. Dahn, A.K. Sleigh, H. Shi, J.N. Reimers, Q. Zhong, B.M. Way, Electrochem. Acta 38 (1993) 1179.
[12] R.A. Nyquist, R.O. Kagel, Infrared Spectra of Inorganic Compounds, Academic Press, New York, 1971.
[13] J.S. Xue, K. Myrtle, J.R. Dahn, J. Electrochem. Soc. 142 (1995) 2927.